

## Crystallographic Analysis of Transition Al<sub>2</sub>O<sub>3</sub> Phases Under the Constrains of Complex Intergrowth and Disorder

Libor Kovarik, Mark Bowden and Janos Szanyi

Pacific Northwest National Laboratory, Richland, Washington, United States

Transition aluminas are heavily used in catalytic applications, both as catalysts and catalytic supports [1]. While much research interest in transition aluminas is naturally directed towards understanding of surfaces and catalytic properties, more basic questions regarding the crystallographic nature of transition aluminas remain a subject of ongoing debate [2-4]. Due to the high degree of structural disorder, and limitation associated with the synthesis of transition aluminas ( $\gamma$ -Al<sub>2</sub>O<sub>3</sub>,  $\delta$ -Al<sub>2</sub>O<sub>3</sub>,  $\theta$ -Al<sub>2</sub>O<sub>3</sub>) in isolated forms, the conventional diffraction approaches cannot be used for crystallography analysis.

In the current study we present a crystallographic analysis of complex structures of  $\delta$ -Al<sub>2</sub>O<sub>3</sub> and  $\theta$ -Al<sub>2</sub>O<sub>3</sub> based on quantitative real-space interpretation of HAADF STEM images in combination with electron diffraction. The HAADF STEM observations were performed with an aberration corrected FEI Titan 80-300.

In the case of  $\delta$ -Al<sub>2</sub>O<sub>3</sub>, we identified the structure as a complex planar intergrowth of four variants. The complexity of intergrowth arises due to the presence of two distinct intergrowth modes, which differ by intergrowth direction and variants selection [4]. An example of the two intergrowth modes, denoted as  $\delta_{1,2}$ -Al<sub>2</sub>O<sub>3</sub> and  $\delta_{2,3,4}$ -Al<sub>2</sub>O<sub>3</sub>, is shown in Figure.1. The first type consists of  $\delta_1$ -Al<sub>2</sub>O<sub>3</sub> and  $\delta_2$ -Al<sub>2</sub>O<sub>3</sub> and the second type consists of  $\delta_2$ -Al<sub>2</sub>O<sub>3</sub>,  $\delta_3$ -Al<sub>2</sub>O<sub>3</sub> and  $\delta_4$ -Al<sub>2</sub>O<sub>3</sub>. The challenges associated with crystallographic analysis come from the difficulty of identifying suitable orientations that are not affected by crystal overlap, and naturally from derivation of full crystallographic parameters from a limited number of zone axis measurements. It will be shown how quantitative analysis of image intensities, local symmetries and phase relationship between the zones enabled us to unambiguously derive the Al and O coordinates in the above described structures. Ab-initio DFT methods have been used for structural refinement. Examples of simulated HAADF images and corresponding crystal structures (only Al are displayed) are included in Figure.1.

The structure of  $\theta$ -Al<sub>2</sub>O<sub>3</sub> has been found to accommodate a different type of structural disorder. It contains a high density of interlinked lattice disorder sites, which break crystallographic periodicity along two principal directions, as shown in Figure 2. The presence of disorder in  $\theta$ -Al<sub>2</sub>O<sub>3</sub> is recognized as a series of high intensity spots in HAADF images. It will be shown that the overall structure can be rationalized as an intergrowth of “ $\beta$ -Ga<sub>2</sub>O<sub>3</sub>” structural type, which was previously considered exclusively for  $\theta$ -Al<sub>2</sub>O<sub>3</sub>, with  $\delta_3$ -Al<sub>2</sub>O<sub>3</sub> motifs that share the periodicity of  $\beta$ -Ga<sub>2</sub>O<sub>3</sub> phase. The structural interpretation together with HAADF simulations of the intergrowth are shown in Figure 2.

As a part of this work we will show how the derived structural models of  $\delta$ -Al<sub>2</sub>O<sub>3</sub> and  $\theta$ -Al<sub>2</sub>O<sub>3</sub> can be used for ensemble level analysis of transition aluminas using recursive stacking XRD approaches [5].

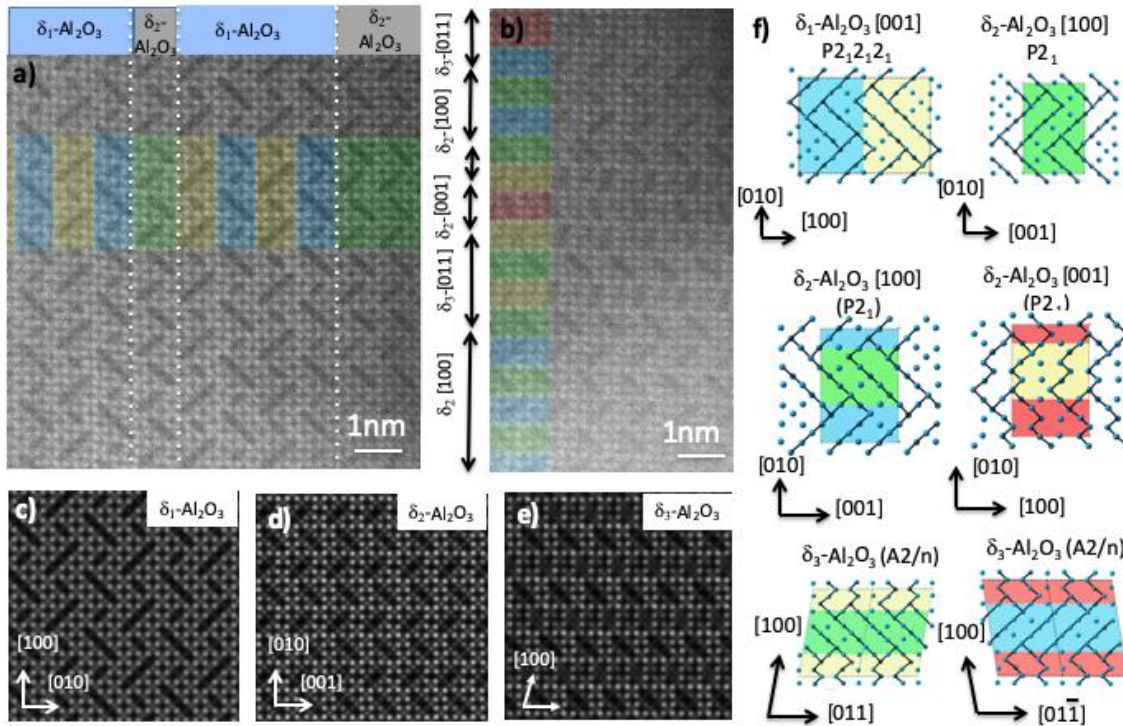


**Figure 1.** (a) Structural intergrowth of  $\delta_1$ - and  $\delta_2$ -Al<sub>2</sub>O<sub>3</sub> as revealed along the cube [100]FCC\_O. (b) Structural intergrowth of  $\delta_2$ - and  $\delta_3$ -Al<sub>2</sub>O<sub>3</sub> as revealed along the cube [100]FCC\_O. (c,d,e) Corresponding HAADF simulations of  $\delta_1$ -Al<sub>2</sub>O<sub>3</sub> and  $\delta_2$ -Al<sub>2</sub>O<sub>3</sub> and  $\delta_3$ -Al<sub>2</sub>O<sub>3</sub>. (f) Crystal projections of  $\delta_1$ -Al<sub>2</sub>O<sub>3</sub>,  $\delta_2$ -Al<sub>2</sub>O<sub>3</sub> and  $\delta_3$ -Al<sub>2</sub>O<sub>3</sub> (only Al displayed).

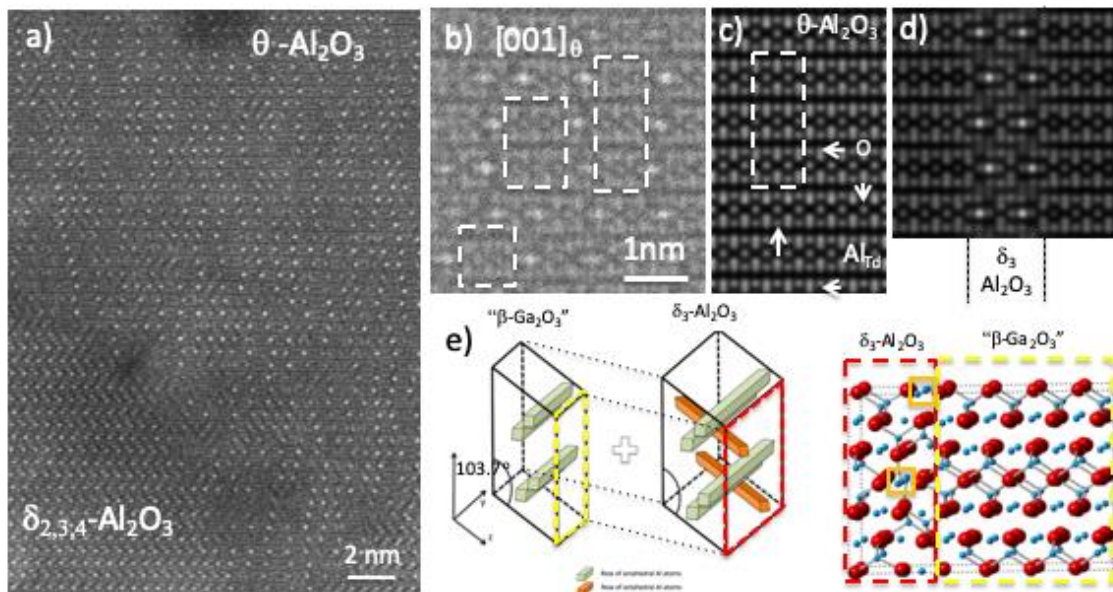


**Figure 2.** (a,b) HAADF observations of microstructural disorder in  $\theta$ -Al<sub>2</sub>O<sub>3</sub>. (c) HAADF image simulation of  $\theta$ -Al<sub>2</sub>O<sub>3</sub> assuming  $\beta$ -Ga<sub>2</sub>O<sub>3</sub> structural type. (d) HAADF image simulation of  $\theta$ -Al<sub>2</sub>O<sub>3</sub> with the intergrowth of  $\delta_3$ -Al<sub>2</sub>O<sub>3</sub>. (e) Crystallographic interpretation of  $\theta$ -Al<sub>2</sub>O<sub>3</sub> structure.

## References

- [1] Busca, G. (2013), *Catalysis Today*, 1–12.
- [2] Kovarik, L., Bowden, M., Genc, A., Szanyi, J., Peden, C. H. F., & Kwak, J. H. (2014). *The Journal of Physical Chemistry C*, 118(31), (2014), p.18051–18058.
- [3] Kovarik, L., Bowden, M., Shi, D., Washton, N. M., Andersen, A., Hu, J. Z., et al.,. *Chemistry of Materials*, 27(20), 7042–7049. (2015)
- [4] Kovarik, L., Bowden, M., Shi, D., Szanyi, J., & Peden, C. H. F., *The Journal of Physical Chemistry C*, 123(14), 9454–9460. (2019).
- [5] This research was performed at Wiley Environmental Molecular Sciences Laboratory (EMSL), a national scientific user facility sponsored by DOE's Office of Biological and Environmental Research and located at PNNL. It was supported by PNNL's LDRD program and the U.S. DOE, Office of Basic Energy Sciences, Division of Chemical Sciences, Biosciences and Geosciences.